Manuscript prepared for Ann. Geophys.
with version 2.3 of the LaTeX class copernicus.cls.
Date: 17 December 2008

Solar Wind Influence on the Driven Electrojet System and the Magnetotail

M. Connors[1], C. T. Russell[2], R. L. McPherron[2], V. Angelopoulos[2], K.-H. Glassmeier[3], G. Rostoker[4], D. Boteler[5], D. Danskin[5], H. Gleisner[6], K. Keika[7], L. Rastaetter[8], and E. Donovan[9]

[1]Athabasca University
[2]IGPP, UCLA
[3]Technische Universitaet Brauschweig
[4]Department of Physics, University of Alberta
[5]NRCan
[6]Danish Meteorological Institute
[7]Space Research Institute, Austrian Academy of Sciences, Graz, Austria
[8]Goddard Space Flight Center
[9]University of Calgary

Abstract. A substorm onset at approximately 10 UT on December 12 2007 was well observed from both the THEMIS constellation and ground observatories in eastern Canada, most emplaced to support the THEMIS project. Clear step-like changes in the solar wind parameters on this day aid in relating them to magnetospheric responses. With the large set of ground magnetometers available, quantitative inversion can be done using the Automated Regional Modelling (ARM) technique which includes both auroral zone and subauroral stations. Not only can the substorm current wedge parameters be well determined, but the response of the driven system morning electrojet to southward IMF during the growth phase can be quantified. A clear subauroral Y component magnetic bay observed in eastern North America before onset can be attributed to this driving, as can stretching at GOES 11 (W) and evening sector bays. The onset appears to have been triggered by a northward turning. Analysis of tail response to the onset must take into account the fact that simultaneously the solar wind northward velocity component reversed from approximately -30 km/s to +40 km/s. The THEMIS C and B spacecraft, located 12 and 14 Re downtail, respectively, showed slow magnetic field X component reversals around the time of onset that are most likely mainly related to the solar wind Vz velocity blowing the tail across the spacecraft, as opposed to direct effects of the substorm. This result is confirmed by MHD modeling and studied using an event-oriented mapping approach.

Keywords. substorms,convection

1 Introduction

The recent increase in numbers of both ground- and space-based observing sites makes quantitative examination of processes during magnetically active periods feasible.

Correspondence to: M. Connors
(martinc@athbascau.ca)

2 Event Overview

The front of a high speed stream arrived at Earth in the early UT hours of Dec. 10, with the solar wind speed ramping up from about 350 km/s to above 400 km/s and densities as much as 25/cc, as shown in Fig. 1. About 1 UT on Dec. 11, this compressed material swept by and the high-speed material arrived, with decreasing density and speed averaging roughly 600 km/s. During the high-speed stream, BZ alternately turned negative and positive, and densities were typically 3/cc. The initial passage was favorable for energization of the magnetosphere (Denton et al., 2008) and the periods of negative BZ with moderate density and high speed were also geoeffective. On Dec. 12 there were many step-like changes in the VZ component of solar wind velocity. Such changes also affect magnetospheric response (Sergeev et al., 2008), and we examine in detail the associated signals observed at spacecraft.

The magnetospheric response to the active solar wind is indicated by the AU and AL indices, and H-SYM, shown in Fig. 2. The slow solar wind speed and non-negative BZ of Dec. 8 resulted in generally quiet magnetic conditions. A long period of moderately southward (averaging -3 nT) IMF in the second half of Dec. 9, with a higher than average density of 6 to 10 /cm3 resulted in AL of about -200 and H-SYM of about -10 nT. Similar conditons early on Dec. 10 resulted in a similar response, with a notable decrease in activity in the latter half of the UT day while the IMF BZ was strongly positive (about +10 nT). An abrupt change to negative IMF BZ, with high densities (15-20 /cm3) and speed of about 450 km/s, resulted in an AL of about -500 and H-SYM of about -30 nT. The short duration of the AL decrease indicates that it was due to subtorm activity, while H-SYM remained at depressed levels for at least two days, indicating

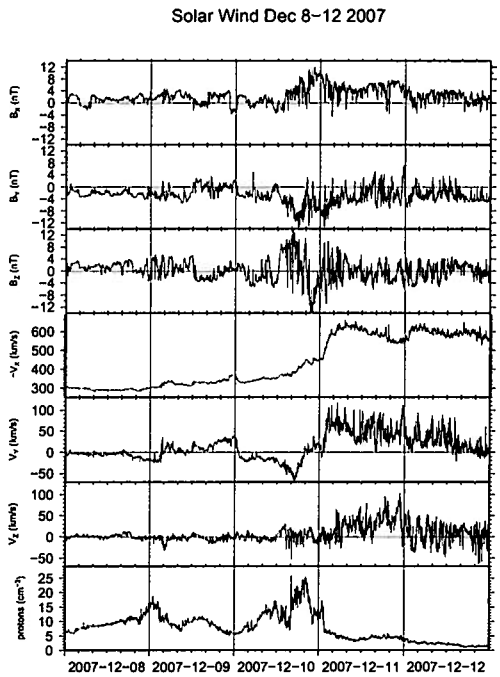

Fig. 1. Solar Wind Parameters from Dec. 8 to Dec 12, 2007. Panels show, from top, GSM magnetic field components BX, BY, BZ, GSM velocity components VX (negated), VY, and VZ, and the ion density. Ticks are at four hour intervals and UT days are separated by vertical lines. Data are from the propagated OMNI database.

a small storm. With high speed and variable BZ, and a near-average density, the solar wind produced constant activity on Dec. 11 and 12. AL repeatedly attained the -300 to -400 nT level, likely due to substorms, with AU, which often indicates evening sector convection, in the 100 to 200 nT range. Grey boxes in the AL/AU panel of Fig. 2 indicate the period of interest on Dec. 12 from 9 to 11 UT. The AU index suggests active convection during this period, the H-SYM indicates a minor storm level, and the abrupt drops in the AL index suggest substorms. The Kp index was close to 3 on Dec. 11 and the first half of Dec. 12, indicating active conditions. The Kp index is also of interest here since it is used to parametrize the Tsyganenko T89C model (Tsyganenko , 1989) used. We will now examine this period in detail.

2.1 Spacecraft and Ground Stations

Both spacecraft and ground stations were well positioned to observe morning and midnight sector phenomena, as may be seen in Fig. 3. European, Greenland, and North American ground stations are now numerous and both auroral zone stations and subauroral magnetometers detected perturbations which we interpret to be associated with the driven system eastward electrojet at a time when the solar wind turned

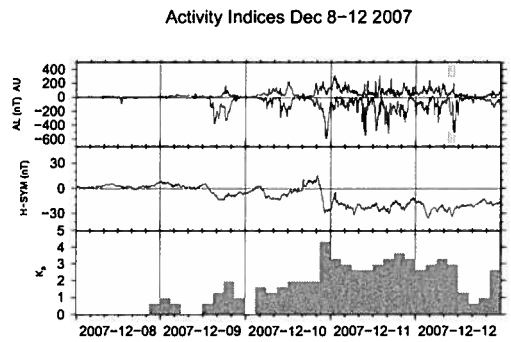

Fig. 2. Magnetospheric response for Dec. 8 to Dec 12, 2007, as indicated by the AU and AL indices (top panel), H-SYM, similar to Dst (bottom panel), and K@-p@- (bottom panel). Time scale and markings as in Fig. 1. Indices are provisional values from WDC for Geomagnetism, Kyoto.

southward. The five THEMIS probes were nominally in the "orbit placement" phase and relatively close to each other in the 2 to 3 MLT sector at radial distances of 10 to 15 Re. GOES 11 was in the midnight sector conjugate to western Canada and Alaska. Both ground station and satellite coverage of the evening sector were sparse. Geotail was in the solar wind approximately 10 Re ahead of the bow shock. At the prevailing solar wind speed (600 km/s), this corresponds to a time delay of 140 s. The excellent positioning of Geotail allowed confirmation of propagation delays in the OMNI data that was also used for the solar wind.

2.2 Event Interval

The event studied here is clearly bounded at its start, 9 UT on Dec. 12, 2007, by a southward turning of the IMF Bz. This led to several characteristic behaviors associated with the substorm growth phase, which will be examined in detail below but which include increase in convection as evidenced by growth of the driven electrojet system, equatorward motion of the electrojets and auroras, and a decrease in magnetic field inclination at geosyncronous orbit. Very close to one hour later, at 10 UT, a northward turning took place and appeared to trigger a substorm in the midnight sector. As shown in Fig. 1, the entire high speed stream period featured step-like changes in the solar wind, and at this time not only the magnetic field changed, but the Z component of velocity. We consider briefly the magnetic activity associated with onset, and by 11 UT the period of interest has ended.

Geotail data was propagated by adding 140 s to the time, and is shown in Fig. 4. BX had a small positive value, dipping to near-zero values in the initial stage of the southward turning. BY had a variable, but small negative value. BZ showed larger variations, from about -5 to +5 nT during the

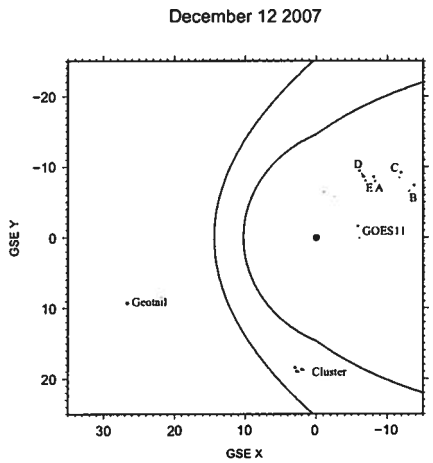

Fig. 3. Positions of spacecraft in GSE coordinates (axis scales in Re) at 9 UT (grey) and 10 UT (black) on December 12, 2007. THEMIS probes are labelled by letters A to E. GOES 11 was in the midnight sector. Geotail (shown only for 9 UT) was in the solar wind roughly 10 Re upstream of the bow shock, which is shown in a nominal position. To the right of the bow shock, the position of the magnetopause (Petrinec and Russell , 1996) for the solar wind conditions at 9 UT is shown. The four Cluster spacecraft were in the magnetosheath as shown at lower right, with a GSE Z coordinate of roughly -9 Re. Earth is to scale, at position (0,0).

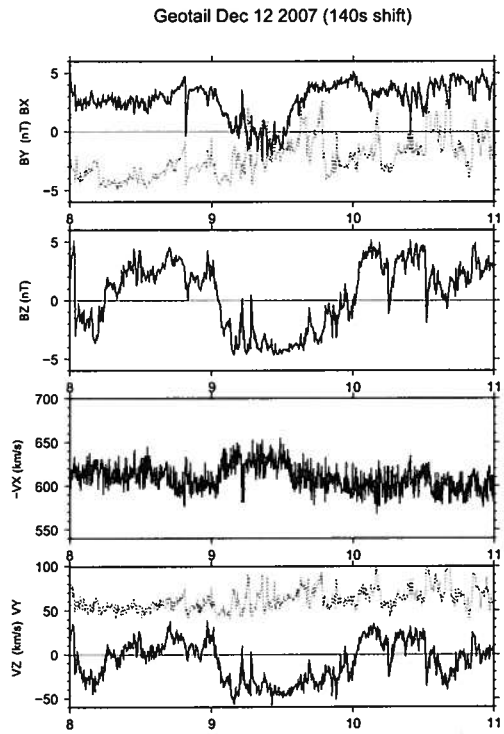

Fig. 4. Geotail data (in GSM coordinates) as propagated to the bow shock by adding 140 s to the time. Top panel shows the BX (solid) and BY (dotted) components of the magnetic field. Top middle panel shows the Z component of the magnetic field. The negative of the X flow velocity component is shown in the bottom middle panel. The bottom panel shows the Y (dotted) and Z (solid) component of velocity. The changes in BZ and VZ between 9 and 10 UT appear responsible for most observed activity.

interval. The southward turning took place at 9:02 UT and the northward turning at 10:02, with variability during the southward interval sufficient to have three brief excursions to slightly northward field. The X velocity was very close to -600 km/s preceding the southward turning. It increased slightly in magnitude, to average about -630 km/s in the initial part of the southward turning period, and about 9:30 UT returned to about -600 km/s. These relatively elevated values could explain pulsations present during this event but not discussed in detail here. VY was in the 50 to 70 km/s range through much of the interval, but with irregular changes and excursions as large as 100 km/s. VZ showed a remarkably high degree of correlation with BZ, notably with an initially negative period just after 8 UT, and an interval with average values of about -40 km/s during the 9 to 10 UT southward turning period. The Geotail values could be confirmed by inspection of the compressed solar wind observed by the four Cluster spacecraft (data not shown), which were located in the magnetosheath. The time delay deduced for Geotail was confirmed in this manner, with the magnetosheath values having a small extra time delay.

2.2.1 Ground Response

The ground response to variations in the solar wind is characterized for the morning/midnight sector auroral and subauroral zones in Fig. 5. Auroral zone stations were baselined by subtracting the average value of measured field components in the hour 16 to 17 UT on Dec. 12, when the A-indices and Kp had returned to minimal values. For subauroral stations, the quiet day of Dec. 8 was subtracted. Due to the relative dominance of Sq at these latitudes, even in December, the simpler procedure appropriate to the auroral zone is not useful. Subtracting a pre-storm quiet day leaves a residual ring current contribution which appears as a negative X bias approximately equal to the H-SYM value appropriate to Dec. 12 as shown in Fig. 2, i.e. about -20 nT. Since the modeling technique described below can include a ring current

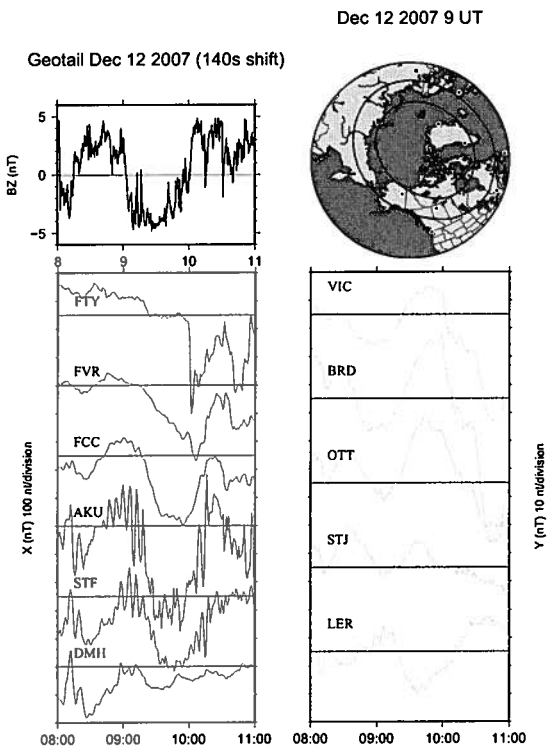

Fig. 5. Propagated Geotail BZ is shown in the top left panel. Below that are traces of the northward component at progressively more easterly stations in the auroral zone, beginning at Fort Yukon near midnight, through stations Fort Vermilion and Fort Churchill in western Canada, Akulivik on the eastern shore of Hudson Bay, Kangerlussuaq (STF) on the west coast of Greenland, and Danmarkshavn on its west coast. The right panel shows subauroral eastward perturbations from corresponding subauroral stations (absent for Fort Yukon). These are Victoria, Brandon, Ottawa, St. John's in Canada, and Lerwick in Great Britain. Positions of these stations are shown on the map at top right, and they are listed west to east in auroral and subauroral zones in Table 1.

bias, no further adjustment was done to the subauroral values. Since the ring current effect is predominantly in X, the Y component perturbations at midlatitudes after subtraction of the quiet day are largely unaffected, as they mainly arise from field aligned current effects.

Although we focus on the response to the solar wind in the 9 to 10 UT period, similar effects may have taken place earlier, as may be seen in Fig. 5. Here the propagated Geotail BZ field is shown and the auroral zone northward component of magnetic field. Focussing on the 9 to 10 UT periods we note that all morning sector stations had a similar response of a negative X bay, starting shortly after the southward turning. At some stations the initial response is masked by pulsations, which seem to have declined in amplitude during the southward field period. Maximimal deviations approached -300 nT. Nevertheless, the -X signatures appear to have started at 10:20 UT at all stations. The midnight sector station Fort Yukon had a minimal negative X bay, and in fact before the southward turning showed the +X effects likely associated with an evening sector eastward electrojet. Sparse station placement in the evening sector during this event does not allow a meaningful study to be done of this current system. This midnight sector station showed very clearly the classic sharp -X bay of substorm onset, at 10:01 UT being very near in time to the northward turning. The most sunward station, in eastern Greenland, showed a subdued but evident X bay during this time. At this station, Y and Z perturbations (not shown) were about the same size as X perturbations, which could be a signature of field-aligned currents nearby. From the auroral zone currents we can form a picture of an westward driven system electrojet stretching from eastern Greenland to Alaska, with maximum current in eastern Greenland. The subauroral perturbations also shown in Fig. 5 are indicative of field-aligned currents. Starting from the west, Victoria is in the meridian of Fort Vermilion, and initially shows a +Y pertubation. This is associated with upward field-aligned current in the auroral zone north of it. Other stations in continental North America also show varying degrees of +Y bays highly correlated with the -X bays, and indicating that the zone of upward net field-aligned current extended all across North America. Only Saint John's, on the island of Newfoundland to the east of North America, had little +D response. This is consistent with its location in the magnetic meridian of western Greenland, where the electrojet current was strongest and had not yet started to bleed away. To complete this picture, perturbations at Lerwick, as a concurrent -Y bay (similar to that seen at all European stations examined) are consistent with net downward field-aligned current in what is inferred to be the most easterly (sunward) part of the driven system electrojet. The consistent picture that emerges is of a three-dimensional electric current system, fed in the late morning sector by currents from space,

Table 1. Station locations

Station	Code	Glon	Glat	Mlon	Mlat
Fort Yukon	FTY	214.8	66.6	261.3	67.3
Fort Vermilion	FVN	244.0	58.4	300.1	64.7
Fort Churchill	FCC	265.9	58.8	327.7	67.9
Akulivik	AKU	281.8	60.8	349.6	70.9
Kangerlussuaq	STF	309.3	67.0	34.8	76.1
Danmarkshavn	DMH	341.4	76.8	101.2	79.3
Victoria	VIC	236.6	48.5	297.0	54.0
Brandon	BRD	260.0	49.9	323.6	58.5
Ottawa	OTT	284.5	45.4	354.7	55.6
St. John's	STJ	307.3	47.6	23.3	57.2
Lerwick	LER	358.8	60.1	88.4	62.1

with an electrojet of variable strength in the auroral zone due to loss of current over a number of hours of local magnetic time. This view of the near-Earth portion of this current system msut be complemented by data from other sources if the origins of the current fed from the magnetosphere are to be understood.

The above discussion has focused on the morning sector driven system. Evidence of the substorm current wedge at auroral latitudes was seen at Ft. Yukon (FTY in Fig. 5) as a sharp decrease in the X component at the onset time of 10 UT. At the most westerly subauroral stations (VIC and BRD in Fig. 5), the +Y bay attributed to field-aligned currents of the morning sector electrojet abruptly ended at the onset time. This signals either the added effects of the downward field-aligned current of the substorm current wedge (a -Y pertubation) or the cessation of the driven system. We will return to this point below. Also prominent at subauroral latitudes is the intensification of -Y perturbation around 10:30 UT. Noting a second intensification in X at this time at Fort Yukon, we include that a second onset took place. Inspection of other data (not shown) allows to conclude that this may have been a poleward border intensification.

2.2.2 Geosynchronous Spacecraft Response

As indicated in Fig. 3, the five THEMIS probes were in the morning sector magnetotail and GOES 11 was in the midnight sector (having replaced GOES 10 as GOES "West" in June 2006). GOES 10 and 12 positions in the morning sector are also indicated (not labelled) but data was not yet available from these spacecraft. Using the Tsyganenko T89C magnetic field model tsyganenko89 and the GEOPACK field line tracing routine, appropriate for Kp=(3-,3,3+), field lines were traced from the positions of GOES and the THEMIS probes to the surface of the Earth, with the results shown in Fig. 6. An advantage of use of this code is the ability to check it online at SSCWEB (sscweb.gsfc.nasa.gov), and unusual values noted locally for THEMIS A (larger than expected BX and BY) were verified to also come from the online code. For the purposes of this work we will not further discuss THEMIS A mapping, but the mappings of the other spacecraft seem generally reasonable, with THEMIS in the morning sector auroral oval and GOES 11 in the midnight sector. The T89C model is based on averaging and is not expected to be accurate under substorm conditions. As seen in Fig. 2, the previous substorm indication from AL was about 6 UT, and the Kp index maintained 3 and 3+ values for several hours before our interval of interest, so use of the T89C model under the stable conditions preceding the 10 UT onset should be justified.

Field values observed at geostationary orbit by GOES 11 are shown in Fig. 7, along with T89C values calculated along the sapcecraft trajectory at the same times. GOES 11 showed known aspects of substorm phenomenology, and also field-aligned current signatures that may be explained in light of

Fig. 6. Footpoint positions of the THEMIS probes and GOES 11, traced using the T89C model. The footpoints for THEMIS probes at 9 UT are labelled with the boxed probe letters A through E, with small dots each 10 minutes leading to a large dot marking the respective spacecraft position at 10 UT. The footprint of the geostationary spacecraft GOES 11 is shown by a boxed letter G, and this spacecraft's position remained within this box during the period discussed. See text for a discussion including the possibly unreliable tracing for THEMIS A.

its position with regard to the morning sector electrojet and the substorm current wedge. The GSM Z component of the magnetic field was approximately 60 nT at 8 UT, near the nominal T89C value during a period of activity Kp=3. GSM BY was near zero, as would be expected near midnight in absence of field-aligned current. The initial GSM BX value of -20 nT is puzzling since one normally thinks of GOES 11 as mapping to the northern hemisphere since it is in the longitude hemisphere containing the north magnetic pole. A partial explanation is the extreme tilt geometry at this time as shown in Fig. 8. Despite being north of the turning point for field lines mapped using T89C, the local field points to -X. For this reason, the inclination exceeds 90 degrees.

Variations at GOES 11 began with an increase in both BX and BZ during the period 8:00 to 9:00 UT, which did not lead to much change in the inclination. At 9:00, corresponding to southward turning, the inclination began to decrease, which in this geometry indicates a more stretched condition. This was mainly due to changes in BX. At 9:20 UT, which has been identified as the beginning of the strengthening of the eastward electrojet, BZ began to decrease and the inclination continued to decrease, which continued until substorm onset at 10 UT, when there was a dipolarization. During this period, BY deviated from the T89C value, with the field be-

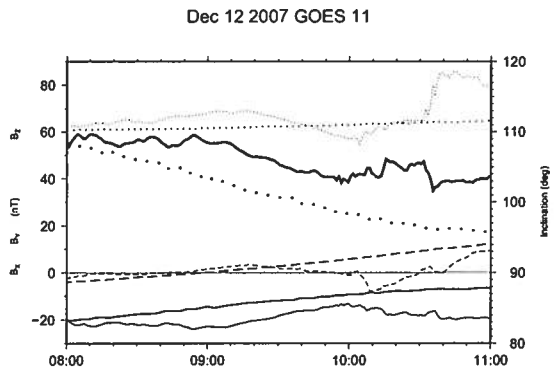

Fig. 7. Temporal variation of the GSM magnetic field observed at GOES 11 (thin lines) and the T89C model field (thicker, generally smoother lines) during the period of interest. BX is shown solid, BY dashed, and BZ dotted, relative to the left-hand scale. The very heavy solid line is the inclination observed, and the large dotted line is that expected from T89C, realtive to the right-hand scale. The large BZ value and near-zero BY are typical of geosynchronous orbit, and the BX value and specific perturbations are discussed in the text.

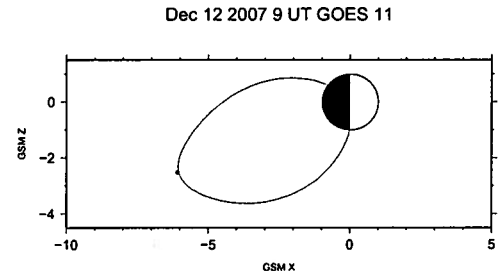

Fig. 8. GSM position of GOES 11 (small dot), shown in the GSM XZ plane (appropriate for the small GSM Y value of -0.6 Rc) at 9 UT on Dec. 12 2007. The field line trace with the T89C model is also shown.

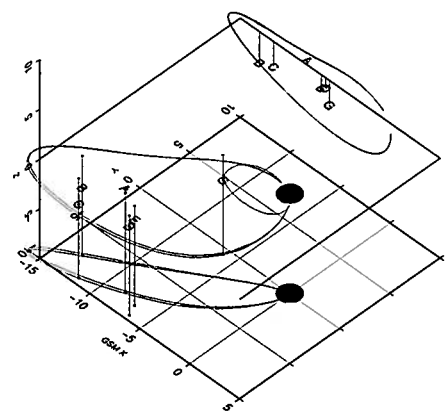

Fig. 9. GSM position of GOES 11 (letter G) at 9 UT and five THEMIS probes at 10 UT (A through E) on Dec. 12 2007. The double field line trace (with the T89C model) originates bracketing the northern hemisphere station Yellowknife, and is close to the inferred location of downward field-aligned current at the time of the 10:30 UT onset. The projection of the Z=0 plane is at the bottom for clarity, with spacecraft positions projected to it be vertical lines. The projection of the Y=0 plane is at the right, with spacecraft offsets in Z marked by vertical lines. Projections of some field lines into these planes are also shown.

coming more westerly. The field became yet more westerly at dipolarization. As indicated above, a second onset took place at roughly 10:30 UT. By this time, the T89C field was becoming more easterly in this coordinate system, but an enhancement of the westerly trend took place. The inclination also appeared to become more stretched, but due entirely to changes in the BZ component, which may not entirely be due to cross-tail field strength,but rather field-aligned currents (see below). Stretching is usually attributed to the cross-tail, and early in the growth phase and at the first onset, it likely played a major role. The changes in BY, however, are most likely initially (from 9:20 to 10 UT) attribuable to being inside the Pedersen current system associated with the morning sector convective electrojet. The fact that they are in the same direction at onset time implies that the perturbations due to the substorm current wedge also include a Pedersen system part.

2.2.3 Morning Sector Tail Spacecraft Response: Growth Phase

The five THEMIS probes were in two groups, with A, D and E being closer to Earth than B and C. This is clear from Fig. 3, and Fig. 9 further shows the distribution in three dimensions and with respect to some magnetic field lines traced using the T89C model. Note that THEMIS A, D, and E were separated by approximately 2 Re in Z, and appear to be above the neutral sheet suggested by the rough symmetry of the T89C field line trace. THEMIS B and C appear to be roughly the same distance as each other below the neutral sheet. We need to examine the magnetic fields themselves (and, further below, the particle data) to verify these conclusions.

The grouping of the THEMIS probes is consistent with the

two similar patterns of magnetic traces shown in Fig. 10. The T89C values are also shown since these are useful in understanding the expected magnetic perturbations under average conditions of about the right level of activity, taking into account the magnetospheric geometry. The inner three probes show a higher Z component value than do the outer two. This may be understood in part due to the natural decrease in Earth's central field with distance. In addition, the value is more than the averaged T89C field. This may reflect a more dipolar condition during this period when IMF BZ was positive. The BY field component at these two probes is positive, also reflecting the influence of the dipole. The positive BY components are less than T89C predicts, and we attribute this to reduced flaring due to high dynamic pressure. The small values of BX suggest a location near the central plasma sheet. The plasma instruments on probes D and E indicate particle energies in the 10 keV range, confirming this. Around 9 UT some pulsation signatures are apparent, and large pulsations were observed on the ground (not conjugate to THEMIS) but we do not further discuss this aspect. During this initial period, the outer pair of THEMIS B and C also showed larger BZ than predicted by T89C. During the growth phase, and especially after 9:20 when effects of the growth phase were manifest on the ground, the main magnetic effect at the A, E, and D inner cluster was in the Y component, toward more positive values (as opposed to GOES which showed more negative values). This trend reversed at 9:35, 9:36, and 9:40 at these respective spacecraft. These perturbations may most readily be explained by a sheet current directed toward +Z GSM, moving inward. At this radial distance such a sheet current would map to the inward FAC of the Pedersen system. Thus the opposite perturbation to that at GOES 11 is explained by the change in +Z direction of the field lines as they go inward, and the reversal of the Z direction (toward -Z) of the current following them. The inward motion is a natural aspect of the growth phase.

To check on the inward motion during this growth phase, we show in Fig. 11 the 630 nm optical observations from a meridian scanning photometer at Gillam (geodetic latitude 56.38). This CGSM instrument's counterpart further north at Rankin Inlet was not operative, so that the poleward limit of the 630 nm emission, which corresponds to precipitation of relatively low energy electrons from the plasma sheet, could not be observed. The equatorward motion of the equatorward border is evident. To attempt to see whether the poleward border also showed similar equatorward motion, we performed a magnetic inversion of the Polaris chain (see Appendix) on the east shore of Hudson Bay (one time zone eastward). The equatorward border as thus deduced showed a good correlation with the 630 nm emission border, upon which it is overplotted. The poleward border did not show much evidence of motion, but the cross-meridian current . The CANMOS station of Fort Churchill (FCC), located north of Gillam, very close to the footpoint of THEMIS C (see Fig. 6) showed evidence of overall motion of the electrojet. The

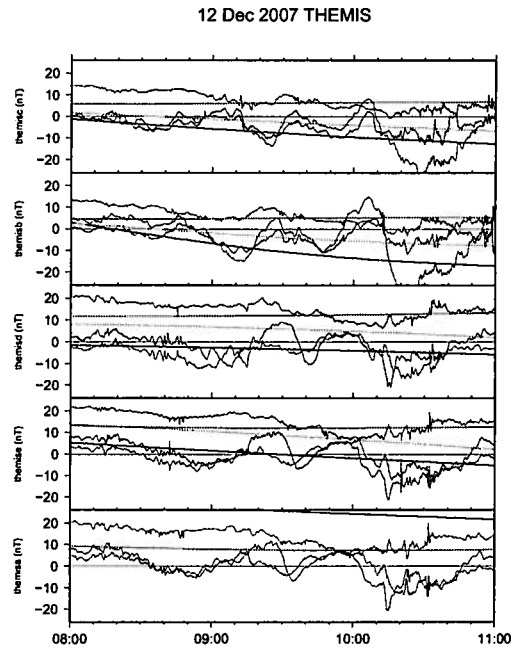

Fig. 10. Magnetic fields observed at the five THEMIS probes from 8 to 11 UT on Dec. 12 2007 are indicated by traces in the colors black, red, and blue, for the X, Y and Z GSM components, respectively. Nearby, smoother traces of the same color (except for THEMIS A) are the corresponding T89C calculated magnetic fields for Kp=3 average conditions.

magnetic inversion of the Polaris chain to the east showed a steady electrojet at the time of the start of inward motion (9:30 UT). The X component at FCC was also steady at this time and shows a very close correspondence to the cross-meridian current as deduced from the Polaris chain. The only cause of change could thus be motion of the electrojet. In the centre of an electrojet, the Z component (verticall down) is 0. Thus, from the southward turning at 9 UT to the start of growth of the driven system electrojet at 9:20 UT, the Z component holding a near-zero value and changing little indicated little motion. This may be confirmed by examination of the optical data, in which the equatorward border of precipitation did not change much (and changes that are evident are due to pulsations). At 9:30 UT, the same time at which motion of the current sheet is inferred (mapping near THEMIS A poleward and eastward of Churchill) the electrojet began to move. We know that the equatorward border moved since that was detected in optical data (total motion 3 degrees). Since the X component mirrored the cross-meridian current (X is at a maximum near the electrojet center and hardly sensitive to motion), the current density above Churchill, and thus the total electrojet width, remained constant. The change in the Z component can only be explained by equatorward motion of the electrojet, so that its poleward border moved equatorward, and this must have also been by

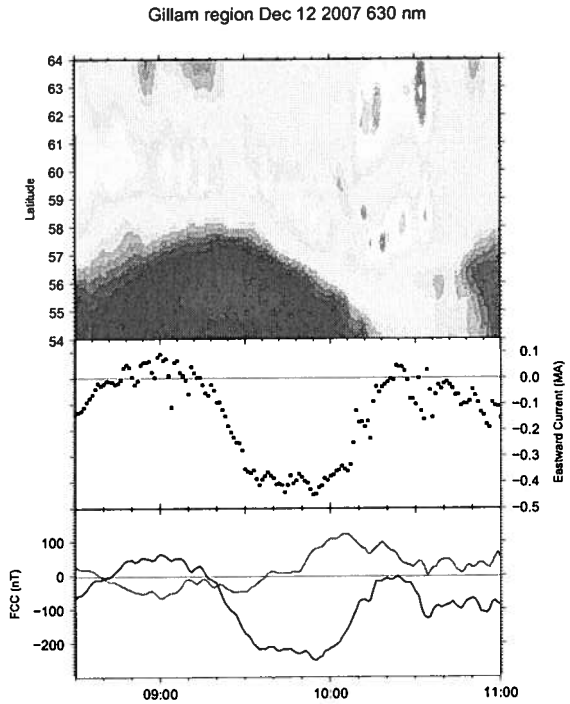

Fig. 11. Optical observations from Gillam from 8:30 to 11 UT on December 12, 2007, in the 630 nm passband, overlain with inversion results from the Polaris East Hudson Bay chain (latitudes indicated by dots). The middle panel shows the total cross-meridian current inferred to exist in the eastward electrojet. The bottom panel shows data from CANMOS station Fort Churchill. The X perturbation is shown in black and the Z perturbation in blue.

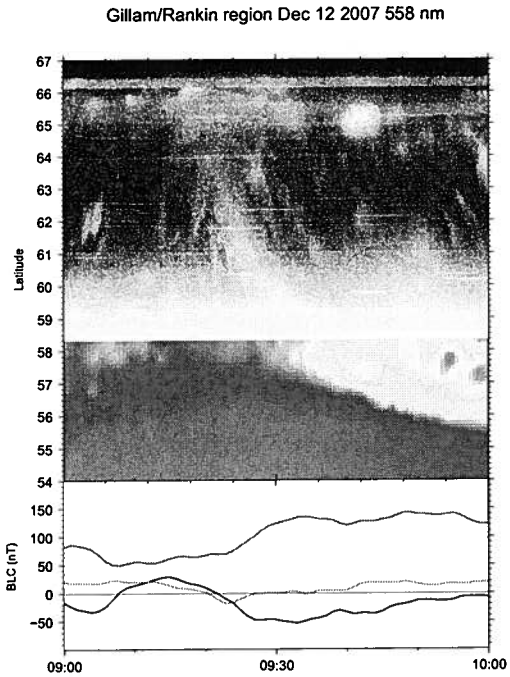

Fig. 12. Optical observations from Gillam from 9 to 10 UT on December 12, 2007, in the 557.7 nm passband, overlain with THEMIS white light keogram from Rankin Inlet. The bottom panel shows data from CANMOS station Baker Lake, near the latitude of Rankin Inlet. The X perturbation is shown in black, Y in red, and Z in blue.

close to 3 degrees. Fig. 12 shows the 557.7 nm emission over Gillam, corresponding to higher energy electron precipitation, with THEMIS white-light imaging from Rankin Inlet (geodetic latitude 62.82) keogram superposed.

The Y component perturbations at the inner THEMIS spacecraft can be explained as the growth of the driven system electrojet's poleward border field-aligned current, followed by equatorward motion. This is entirely consistent with magnetic and optical observations near the foot point. After this inward motion took place, the X and Y spacecraft components at the inner set of spacecraft tracked each other, and we attribute their coupled motion to vertical motion of the current sheet. This behavior was seen at the outer pair of THEMIS B and C at all times during the growth phase, and once the field-aligned current passed inward of the inner spacecraft, they shared this "tail-like" characteristic.

Another aspect of the change to tail-like characterisitics is shown in Fig. 13, Fig. 14, and Fig. 15. The first of these shows "outer" spacecraft THEMIS C particle data from xx to XX eV. At 9:30 UT there was an increase in flux and temperature. The next two show THEMIS D and E particle data. Before 9:30 UT there was a low energy component which corresponds to the low-energy particle sheet precipitation causing the 630 nm emission shown in fig. 11. After 9:30 UT, this component was no longer present at either spacecraft, and the average temperature increased. With the inward motion of the electrojet, its northern border field-aligned current moved in past the spacecraft. At this time, the low energy particles associated with precipitation into the electrojet region (i.e. the auroral oval) were no longer present at the spacecraft.

We have shown that a change in character in the morning tail took place when the growth phase driven system became active.

2.2.4 Spacecraft Response to Substorm Onset

As shown in Fig. 5, substorm onset on the ground produced very clear signatures in the Alaska meridian, with the time of onset deduced to be 10:01 UT based on a very sharp X bay observed at Fort Yukon. Low latitude stations in western North America, which had shown a positive Y bay associated with upward field-alingned current from the westward driven system electrojet, showed an abrupt change to a negative Y bay, associated with the downward current of the midnight sector substorm current wedge. The onset appeared to be

closely related to a northward turning of the solar wind magnetic field as observed at Geotail, just upstream of the bow shock.

The GOES 11 spacecraft was in the midnight sector (Fig. 3) and depression of its Y and Z magnetic components (Fig. 7) was explained above as due to the Pedersen system of the morning sector electrojet, and the growth of the cross-tail current, respectively. At onset, the Y component decreased further, the Z component relaxed to the T89C level appropriate for the activity level, and the X component became more negative, which in this geometry indicates less tail stretching (Fig. 8). The changes in the X and Z components are classic dipolarization signatures (once the unusual geometry is accounted for). The further decrease in Y component indicates that the Pedersen system associated with the susbtorm current wedge had an intensified current, with GOES 11 remaining inside the mapping of the current wedge electrojet (i.e. between Region 1 and Region 2 field-aligned currents similar to those associated with the morning sector). At 10:30 UT, an 'overdipolarization' is seen in the form of a large increase in the Z component. We regard this as the end of the first onset period and discuss its cause below.

At the inner set of THEMIS probes (A, D, and E) both the X and Y GSM components decreased at onset (10:01 UT), with the Z component remaining unchanged. In the minutes preceding onset, the X component had increased to be positive compared to T89C values (at probes D and E; A T89C values appear unreliable as discussed above; below, any reference to T89C and spacecraft will imply only D and E probes). We do not explain this increase here, but in conjunction with particle data shown in Fig. 14 and Fig. 15, take it as an indication that the probes were in the northern plasma sheet. The decrease at 10:01 UT brought the X value to near T89C values and appears to place the spacecraft in the centre of the plasma sheet. At 10:12 UT, the X and Y values abruptly decreased further, with Y eventually reversing before X reached its minimal value. We take this as evidence of an excursion into the southern plasma sheet. In this period of 10:01 to 10:12 UT, the higher energy particles at THEMIS D and E dropped out as seen in Figures 14 and 15 (at THEMIS A also; its low energy detector was not operative). At 10:12 the temperature moments at D and E also rapidly declined.

To understand the perturbations at THEMIS B and C, the geometry near the near-Earth neutral point must be used as opposed to a planar tail geometry. We infer that the neutral line was at approximately X=-15, i.e. slightly further downtail than the spacecraft. Flow bursts, likely emanating from the reconnection region at the time of onset, moved the position of the thinned portion of the plasma sheet inward at the spacecraft position. In this way, THEMIS B appeared to move from the north plasma sheet, as indicated by magnetic and particle data above, into the south plasma sheet boundary layer, with nearly lobe-like field. THEMIS C did not make as large a traversal, and effects observed there, although similar, were smaller. We first examine the flow

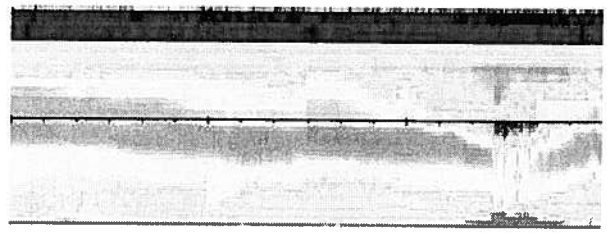

Fig. 13. THEMIS C particle data from 8 to 11 UT on December 12, 2007.

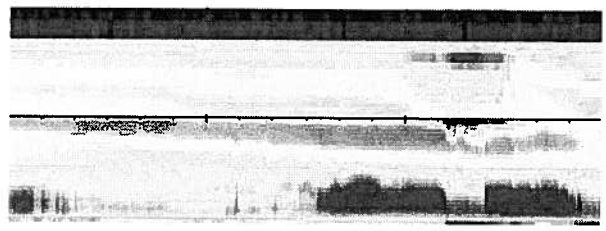

Fig. 14. THEMIS D particle data from 8 to 11 UT on December 12, 2007.

bursts, which are shown in Fig. 16. Flows of order 100 km/s first appeared at the onset time of 10 UT, and are in the Y component as observed at THEMIS B. Due to the geometry of the neutral line being to first order invariant along Y, we do not expect changes with respect to the relative position in the magnetotail due to these flows, nor are such changes observed. At 10:10 UT, an Earthward-directed and larger (nearly 200 km/s) flow burst was observed at THEMIS C, which should have been nearer the plasma sheet than THEMIS B, with a corresponding similar burst of smaller magnitude at THEMIS B. We regard this Earthward burst as being responsible for tail reconfiguration. In addition, at the time of this burst, the Z velocity briefly approached +50 km/s at both spacecraft (data not shown). This would have the effect of moving the tail upward and the effective spacecraft positions downward.

The thinned tail region downtail of the spacecraft is indicated schematically in Fig. 17. The initial positions of THEMIS B and THEMIS C are shown, with both north of the plasma sheet. The X-component flows, which were Earthward, would have carried in or elongated the thinned region near the reconnection site. As illustrated schematically, this would have the effect of moving THEMIS C effectively southward within the plasma sheet, and THEMIS B into the boundary layer or edge of the lobe. These effective motionss have been plotted as new spacecraft positions in the figure; however it is the plasma sheet and reconnection region which have moved (downward and leftward in the figure) with respect to the spacecraft, which on this timescale are essen-

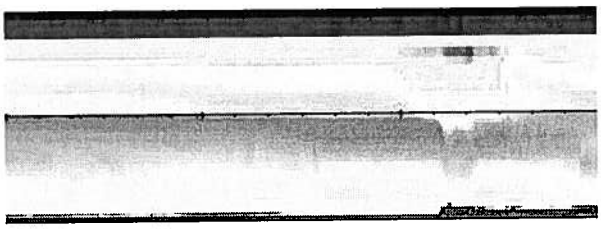

Fig. 15. THEMIS E particle data from 8 to 11 UT on December 12, 2007.

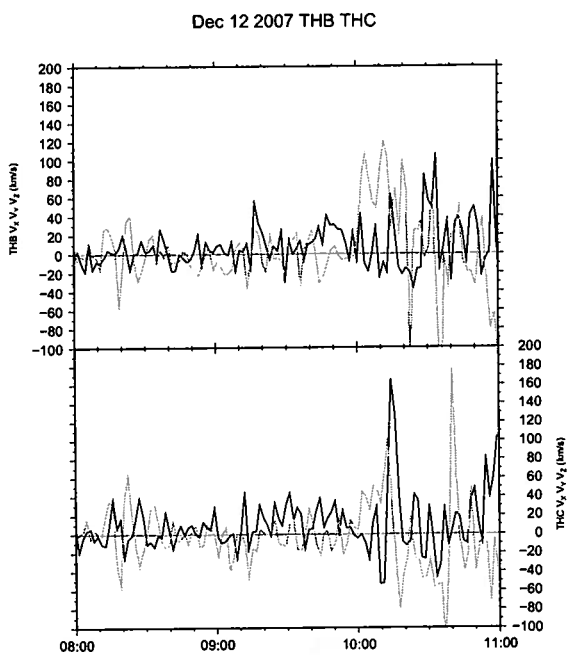

Fig. 16. GSM VX and VY velocities observed at THEMIS B and THEMIS C from 8 to 11 UT on December 12, 2007. VX is indicated by black traces, and VY by red traces.

tially stationary.

2.2.5 Second Onset

As noted above, the midnight sector evidence for a second onset is the 'overdipolarization' at GEOS 11 along with increased magnitude of X component perturbations on the ground, at higher latitude than the 10:01 onset. In addition, Y component ground perturbations increased in magnitude (becoming strongly negative in western North America) at this time. We infer that a strong field-aligned current existed in the sector of THEMIS B and C. The perturbations in the southern magnetosphere which they detected (increase in X component) can in part be explained by inward FAC in the southern hemisphere, but may also result from current sheet

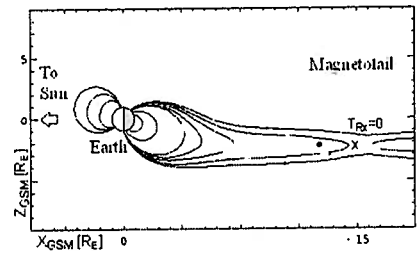

Fig. 17. Quasischematic view of tail showing relative apparent motion of THEMIS B (dark red dot) and THEMIS C (green dot) at a time after inward flows moved THEMIS B nearly into the south lobe and moved THEMIS C south of the current sheet. Initial positions are shown by larger dots, and final effective positions by smaller dots. The change in effective position is due to motion of the current system.

motion. The Z perturbation at GOES is due to inward FAC in the northern hemisphere which is east of the spacecraft position.

3 Appendix: Forward Modeling

Automated Forward Modeling proposes a forward model of current systems which could give rise to the magnetic perturbations observed. The parameters in that model are varied in such a way that the deviation between the observed magnetic fields and those predicted by the model are reduced. In the ideal case, the parameters can be chosen to correspond to simple physical parameters associated with the current system. A forward model can be made using the Biot-Savart law in combination with Earth induction, by specifying where currents flow in space and the ionosphere Kisabeth and Rostoker (1977) Kisabeth (1979). Adjustment of the parameters specifying the current system can be done until the match to the input data is optimal. In principle, arbitrarily complex current systems may described in three dimensions in near-Earth space and their parameters determined. In practice, the method works best with simple systems with few parameters. A useful form is Automated Meridian Modeling (AMM) in which all of the stations lie in a meridian, and the current system is composed of a simple east-west aligned electrojet whose borders and total (cross-meridian) current are determined. Another simple form is Automated Regional Modeling (ARM), in which both auroral zone and subauroral perturbations are used, but in a restricted region, usually one in which there are many stations to contribute data. If the latter condition is met, this version can determine the longitudinal extent of current systems. Due to the sparse distribution of magnetic stations, general use of the full AFM technique on a global scale is not often possible as there is not sufficient constraint.

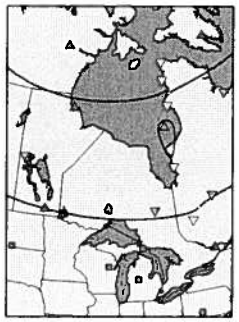

Fig. 18. New stations of the AUTUMN/CANMOS/Polaris collaboration are shown with inverted white squares and their locations are given in Table 2. Other symbols indicate CANMOS Canadian federal government (NRCan) sites (red triangles), THEMIS GBOs (inverted pink triangles), and THEMIS GEONS (red squares), whose locations may be found elsewhere.

Table 2. Station locations

Station	Code	Glon	Glat	Mlon	Mlat
Val d'Or	VLDR	-77.5	48.1	352.1	58.3
Wemindji	WEM	-78.8	53.0	349.9	63.1
Inukjuak	INU	-78.1	58.45	350.1	68.6
Akulivik	AKU	-78.2	60.8	349.5	70.9
Ivujivik	IVU	-77.81	62.42	349.8	72.6

4 Conclusions

We have found that the growth phase morning sector current system could be well approximated by a region of downward current in the auroral ionosphere, a westward electrojet, and distributed upward current over much of North America. This allowed a good representation of magnetic perturbations at auroral and subauroral latitudes. A geometrically similar system formed at the time of substorm onset, but in the midnight sector, having the simple characteristics of the substorm current wedge. This system allowed good representation of near-midnight magnetic perturbations in the auroral and subauroral zones. Magnetic perturbations at THEMIS spacecraft conjugate to the driven system electrojet during the growth phase could be represented by field-aligned currents associated with electrojets, changing as the electrojet moved equatorward. At substorm onset, changes at the spacecraft appear to have been largely due to motion of the tail produced by the Z component of solar wind velocity, and this effect must be considered in attempting to understand variations seen at spacecraft at such times.

Acknowledgements. We wish to thank the World Data Center for Geomagnetism, Kyoto, for Provisional AE and SYM-H indices, and the National Space Science Data Center for propagated OMNI solar wind data. Several datasets were obtained through the NASA CDAWeb system, and positions through SSCWEB. The NSSDC OMNI data was prepared by J.H. King and N. Papatashvilli. We acknowledge the DARTS system at ISAS (http://darts.isas.jaxa.jp/stp/) and the help of Professors T. Nagai and Y. Saito in obtaining Geotail data. Alaska Chain magnetic data was supplied by the Geophysical Institute of the University of Alaska. The AUTUMN chain received initial funding from the Canada Foundation for Innovation, and we thank Rob Irwin and Northern Lakes College for facilitating some sites. The CANMOS and Greenland magnetometers are financed by the national governments of Canada and Denmark, respectively. European subauroral data was obtained through Intermagnet, and we thank the contributing observatories as well as that organization. The Polaris chain was established with the kind assistance of David Evans, now at the University of Calgary. Cluster data from CDAWeb was used, for which we acknowledge A. Balogh of ICSTM. We thank N. Tsyganenko for his T89C code and GEOPACK tracing software, available both as source code which we implemented, and at SSCWEB. GOES data is used courtesy of H. Singer of NOAA. The GMT plotting package of Wessel and Smith has proved invaluable. We thank the THEMIS team and in particular Jim McFadden for particle measurements. THEMIS was made possible by NASA under NASA grant NAS5-02099. We acknowledge the contributions of DLR under contract 50 OC 0302 for the FGM instrument and the CSA for the installations of the THEMIS/GBOs in Canada. KHG was financially supported by the German Zentrum fuer Luft- und Raumfahrt under grant 50QP0402. Some of the work was done while MC was a guest at STELAB, for which he thanks K. Shiokawa, and where he benefitted from discussions with the group of T. Kikuchi, in particular with Y. Nishimura. MC has support for this work from NSERC and the Canada Research Chairs.

References

Denton, M. H., and J. E. Borovsky (2008), Superposed epoch analysis of high-speed-stream effects at geosynchronous orbit: Hot plasma, cold plasma, and the solar wind, J. Geophys. Res., 113, A07216, doi:10.1029/2007JA012998.

Kisabeth J. L., and G. Rostoker, Modeling of the three-dimensional current systems associated with magnetospheric substorms, Geophys. J. R. astr. Soc. 49, 655-683, 1977.

Kisabeth, J. L., On Calculating Magnetic and Vector Potential Fields due to Large-Scale Magnetospheric Current Systems and Induced Currents in an Infinitely Conducting Earth, in Quantitative Modeling of Magnetospheric Processes, edited by W. P. Olson, American Geophysical Union, Washington, pp. 473-498, 1979.

Petrinec, S. M., and C. T. Russell (1996), Near-Earth magnetotail shape and size as determined from the magnetopause flaring angle, J. Geophys. Res., 101, 137-152.

Sergeev, V. A., N. A. Tsyganenko, and V. Angelopoulos,Dynamical response of the magnetotail to changes of the solar wind direction: an MHD modeling perspective, Ann. Geophys., 26, 2395-2402.

Tsyganenko, N. A. (1989), A magnetospheric magnetic field model with a warped tail current sheet,Planet. Space Sci. 37, 5-20.